IEEE Access
Multidisciplinary | Rapid Review | Open Access Journal

IEEE POWER & ENERGY SOCIETY SECTION

Received 2 March 2024, accepted 18 March 2024, date of publication 28 March 2024, date of current version 4 April 2024.

Digital Object Identifier 10.1109/ACCESS.2024.3382715

RESEARCH ARTICLE

A Novel Control Scheme of Four Switch Buck-Boost Converter for Super Capacitor Pre-Charger

HYEON-JUN KWON[1], KU-YONG KIM[2], AND JUN-HO KIM[3], (Member, IEEE)

[1]Department of Electrical and Electronic Convergence System Engineering, Keimyung University, Daegu 42601, Republic of Korea
[2]MDM, Daefu 42702, Republic of Korea
[3]Department of Electrical Energy Engineering, Keimyung University, Daegu 42601, Republic of Korea

Corresponding author: Jun-Ho Kim (junho.kim@kmu.ac.kr)

This work was supported in part by Korea Evaluation Institute of Industrial Technology (KEIT), South Korea, Grant funded by the Ministry of Trade, Industry and Energy (MOTIE), South Korea, High Density Power Module and High Power Density Power Conversion Technology Development of Vehicle, under Grant 20019073.

ABSTRACT This paper presents the novel control method of the Four-Switch Buck-Boost (FSBB) converter for Super Capacitor Pre-Charger (SCPC) in hydrogen electric vehicles. The method is proposed to improve voltage regulation characteristic during super capacitor pre-charging, and is able to maintain continuity of duty ratio and voltage conversion ratio. The novel control scheme uses two independent duty ratio, and one varies while the other is fixed in whole operation. The duty ratio of changing the value changes at the transition point. Even though operation mode changes for achieving unity voltage gain, the additional switch state diminishes voltage fluctuation at transition point compared to conventional method. Also, the size of passive components can be reduced. The feasibility of the proposed control method is substantiated through simulation and experiment with 10kW prototype.

INDEX TERMS Four-switch buck-boost (FSBB), hydrogen fuel cell electric vehicle (HFCEV), open circuit voltage (OCV), super capacitor pre charger (SCPC).

I. INTRODUCTION

Since the concerns about climate change caused by fossil fuels, the adoption of electric vehicles (EVs) is accelerating in worldwide [1], [2]. With the proliferation of EVs, problems related to carbon emissions from fossil fuels can be alleviated. EVs can be powered in several ways such as converting kinetic energy to electrical energy in the powertrain, using internal combustion engines, or utilizing hydrogen fuel cells. The power generated from hydrogen fuel cells can cause voltage fluctuations when load changes. In the HFCEV system, it is possible to minimize voltage fluctuations by configuring a supercapacitor as shown in **FIGURE 1** [3], [4].

The voltage of the super capacitor approximates 0V, when a HFCEV is in initial state. Without SCPC, inrush current can occur due to the voltage difference between the super capacitor and the hydrogen fuel cell. This current can lead to shortened lifespan of the super capacitor and failure of the hydrogen fuel cell [5], [6]. The method to limit the inrush current are as shown in TABLE 1. The resistor type is simple and robust. However, it takes long charging time, and has low power-to-weight ratio. The higher charging current not only shortens charging time, but also increases conduction loss in resistor. Thus, additional cooling system is required, which cause power-to-weight ratio becomes lower. The DC-DC converter type has higher efficiency than resistor type, and has faster charging time because of high charging current. In fact, DC-DC type needs more complex structure and control than the resistor type. However, DC-DC type can achieve high power density (size), fast charging speed, and low energy loss. Therefore, the DC-DC type can be adopted for SCPC in HFCEV. There are several kinds of topology can be chosen for SCPC. In this paper, the FSBB topology is used.

The required specifications are as follows:

The associate editor coordinating the review of this manuscript and approving it for publication was K. Srinivas.

TABLE 1. Comparison of two SCPC types.

Comparison	Resistor type	DC-DC converter type
Block diagram	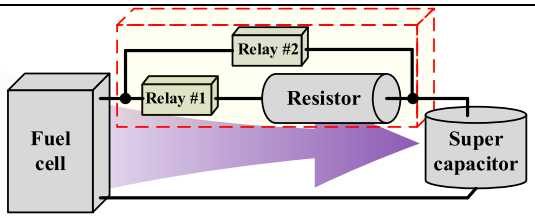	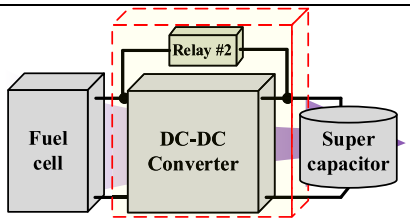
Structure	Simple	Relatively complex
Power density	Low	High
(Size)	(Large)	(Small)
Charging speed	Slow	Fast
Power loss	Large	Small

TABLE 2. Comparison of SCPC specifications and characteristics.

Parameters	SCPC spec	FSBB	Buck	Buck-Boost
Voltage conversion ratio	$0 \leq G \leq 1$	$0 \leq G \prec \infty$	$0 \leq G \prec 1$	$-\infty \prec G \leq 0$
Polarity of output voltage	Positive	Positive	Positive	Negative
Isolation type	None	None	None	None

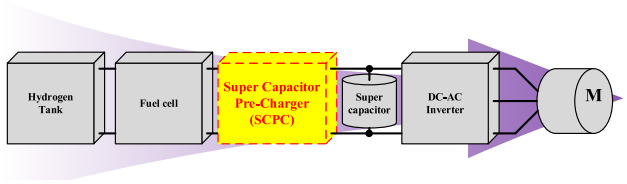

FIGURE 1. The powertrain structure of a hydrogen electric vehicle.

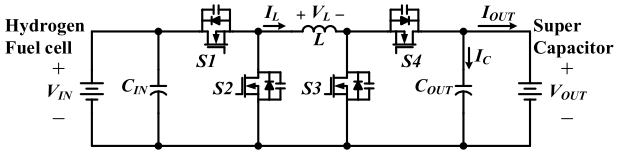

FIGURE 2. FSBB converter circuit diagram.

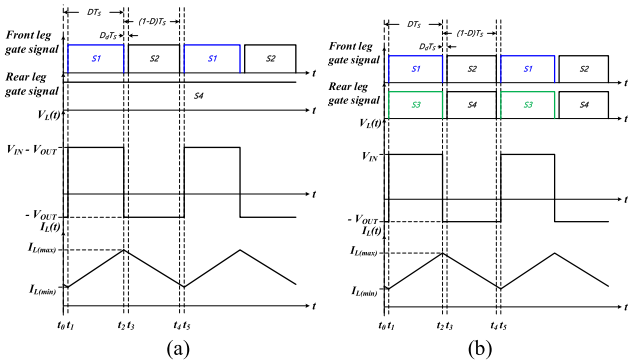

FIGURE 3. Analysis of the operating waveforms of the FSBB converter with the conventional control method (a) Buck operation, (b) Buck-boost operation.

- Voltage gain from 0 to 1.
- Same polarity between input and output voltage
- Continuous connection of ground pattern.

The above conditions are because of the following reasons. At first, it is appropriate that the charging operation ends when the super capacitor voltage is equal to the hydrogen fuel cell voltage. If it is not met, high inrush current flows through Relay #2 when it turns on. Due to these characteristics, step-up operation is required [7], [8]. Second, the input and output side of the SCPC becomes the same node when Relay #2 turns on. Thus, it is required to have the same polarity. Lastly, the ground pattern is continuously connected as same as resistor type. Thus, a non-isolated DC-DC converter is required. As a result, FSBB converter is suitable as shown in TABLE 2.

FSBB converter's circuit diagram is described in **FIGURE 2**. It can operate in three different topologies through the combination of gate operations of from S1 to S4. The combination allows FSBB to operate as buck, boost, and buck-boost. When FSBB charges a super capacitor, it is possible to use only the buck-boost operation or utilize buck then buck-boost operation. Relationship between the average inductor current (I_L) and the output current (I_O) in the buck-boost operation can be expressed by Eq (1). According to Eq (1), the average inductor current is always larger than the output current in the buck-boost operation. However, in the case of buck operation, the average inductor current is equal to the output current.

$$I_L = \frac{I_O}{1 - D} \tag{1}$$

If only buck-boost operation is used, FSBB has higher energy loss compared to using both buck and buck-boost operation. Because, inductor current in buck-boost operation is larger than inductor current in buck operation. Therefore, in order to minimize the energy loss, buck operation should be

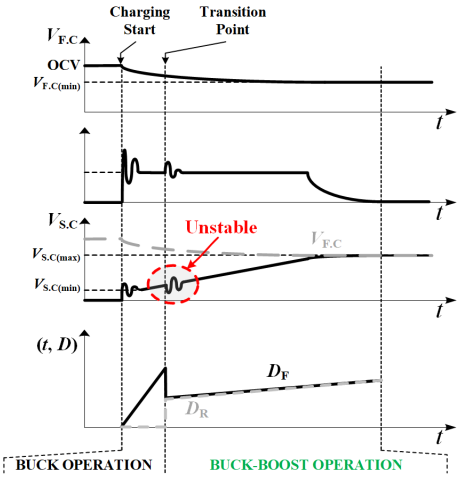

FIGURE 4. Charging operation waveform of the conventional control method.

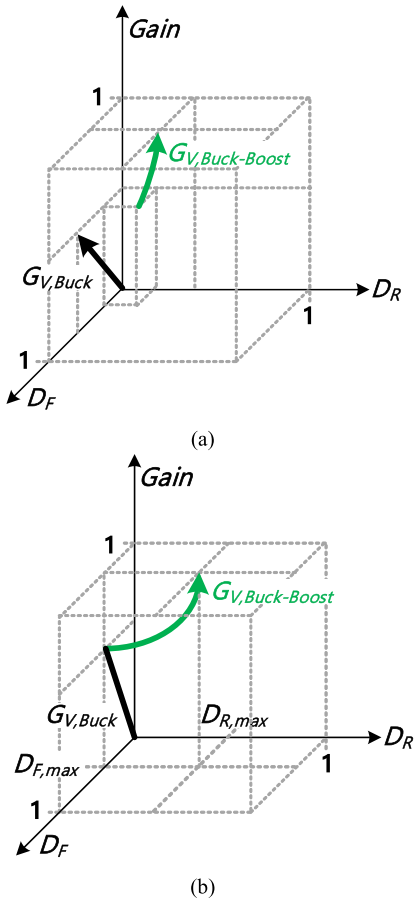

FIGURE 5. Comparison with two gain curve that are conventional and proposed control methods (a) Gain curve with conventional control method, (b) Gain curve with proposed control method.

used as much as possible. After buck operation, buck-boost operation should be used.

The operating waveforms of the FSBB converter with conventional control are depicted in **FIGURE 3**, as shown in (a) and (b). **FIGURE 3** (a) illustrates the operation in buck mode, while (b) shows the operation in buck-boost mode. The FSBB converter operates in buck mode initially to charge the super capacitor during the ignition phase.

$$G_{V,Buck} = \frac{V_{OUT}}{V_{IN}} = D_F - D_d \tag{2}$$

$$G_{V,Buck-boost} = \frac{V_{OUT}}{V_{IN}} = \frac{D_F - D_d}{1 - D_F - D_d} = \frac{D_R - D_d}{1 - D_R - D_d} \tag{3}$$

When the super capacitor voltage approaches the critical threshold voltage chosen by designer, FSBB will change from buck mode to buck-boost mode.

The FSBB converter can be operated as buck, boost, buck-boost converter. With duty cycle D, the voltage conversion ratio is D, $1/(1\text{-}D)$, $D/(1\text{-}D)$, respectively. However, there are several problems with conventional control method subscribed. Therefore, this paper analyzes the problems of the conventional control method of the FSBB converter in part II. To overcome these problems, a novel method is proposed. The validity is evaluated by simulation and experiment.

II. CONVENTIONAL CONTROL METHOD

In conventional control method, *S1* and *S3* are controlled by the same duty ratio, D. For analysis, D_F and D_R are used instead of D, and both are duty ratio for *S1* and *S3* respectively. In **FIGURE 4**, the waveform represents fuel cell output voltage, current flowing through the super capacitor (charging current), super capacitor voltage, and duty cycle from top to bottom. As shown in the figure, voltage ripple occurs at transition point with conventional method [9], [10]. It can be analyzed as shown in **FIGURE 5 (a)**. The relationship between duty ratio and voltage conversion ratio, $G_{V,Buck}$ and $G_{V,Buck-boost}$, can be obtained through flux-balance from the inductor voltage waveform $V_L(t)$ shown in **FIGURE 3**. Thus, the relationship can be expressed by Eq. (2) and (3). During the buck-boost operation, the D_F and D_R are the same value. Because of it, there is nonlinearity of $G_{V,Buck}$ and $G_{V,Buck-boost}$ curve. Due to the characteristic, the output voltage of the FSBB converter at the transition point becomes unstable [11].

The discontinuity is the control obstacle at the transition point [11]. Also, this discontinuity can cause derangement of output voltage [12]. There are several approaches to solve the problem such as phase shifting PWM scheme [13], [14], pseudocritical control method [15], and model predictive control [16]. Those methods are suitable to achieve wide voltage gain since they focused on resolving discontinuities in the mode change between buck and boost operations. However, unity gain is required as maximum value for SCPC. Thus, a simple method is required to resolve the discontinuity between buck-boost and buck operations. The novel control scheme is required that $G_{V,Buck}$ and $G_{V,Buck-boost}$ have the same magnitude at the transition point. Therefore, to obtain the same voltage gain at the transition point, it has a characteristic of being linear in voltage gain as shown in **FIGURE 5 (b)**.

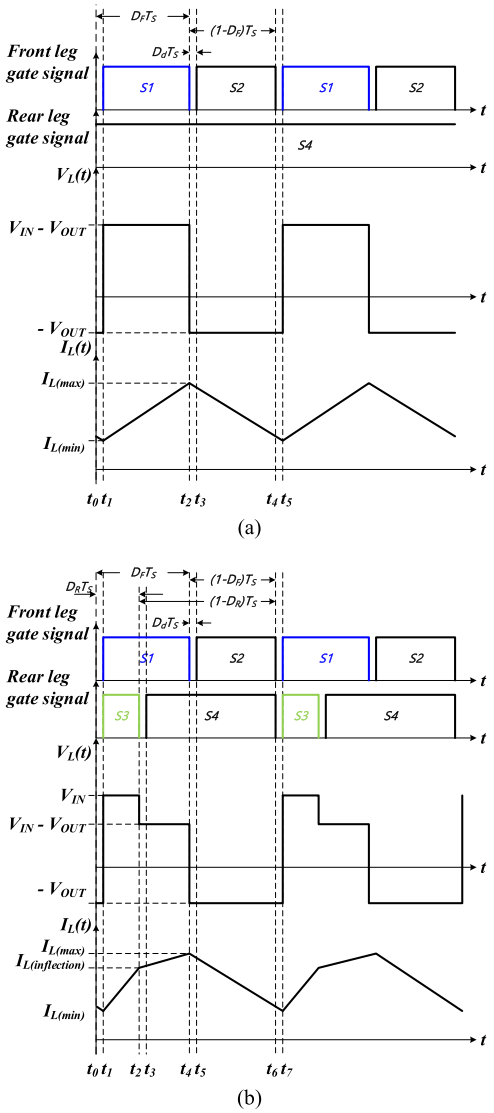

FIGURE 6. Analysis of the operating waveforms of the FSBB converter with a novel control method (a) D_R is zero, (b) D_R is not zero.

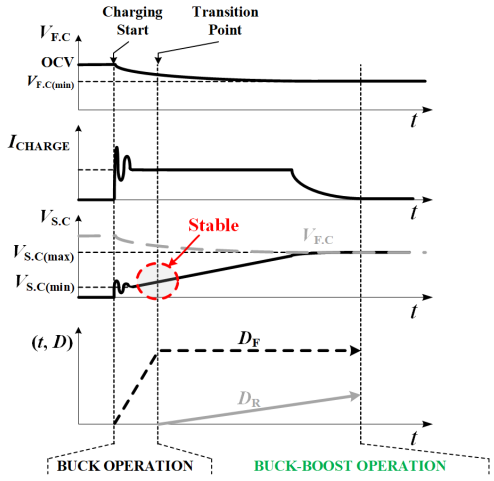

FIGURE 7. Charging operation waveform of the proposed control method.

III. PROPOSED CONTROL METHOD

A. CONCEPT OF THE PROPOSED CONTROL METHOD

In order to overcome the voltage ripple issues when transitioning from buck operation to buck-boost operation, linearity between $G_{V,Buck}$ and $G_{V,Buck-boost}$ should be required at the mode transition point. So, in order to obtain linearity of output voltage, the duty cycle for *S1* and *S3* need to be independent and appropriately adjusted to form this continuity.

In other words, D_F and D_R are used as duty ratio for *S1* and *S3*, respectively. The operating waveform of the FSBB converter with the proposed control method is depicted in **FIGURE 6**. **FIGURE 6** (a) and (b) depict the waveforms during buck operation and buck-boost operation. When D_R is zero, FSBB converter operates as buck converter and when D_R is larger than zero, FSBB converter operates as buck-boost converter. The operation of the proposed control method at $D_R = 0$ remains the same as the buck operation in conventional control method. D_F increases linearly from initial startup to transition point. After buck operation has ended, D_F is fixed and D_R increases linearly from transition point to end of charging. In summary, through the proposed control method, output voltage of FSBB converter should be stable in transition point as shown in **FIGURE 7**. Because D_F and D_R increase linearly as shown in **FIGURE 5** (b).

The proposed control method has a total of six operating modes. The time intervals t_1-t_2 in **FIGURE 6** (b) represent **Mode 1**, t_2-t_3 is **Mode 2**, t_3-t_4 is **Mode 3**, t_4-t_5 is **Mode 4**, t_5-t_6 is **Mode 5**, and t_6-t_7 is **Mode 6**. In **Mode 1**, S1 and S3 are turned on, while S2 and S4 are in the off state. At this time, the current path is formed as shown in **FIGURE 8** (a). The terminal voltage of inductor becomes V_{IN}. Since $V_{IN} > 0$, the current flowing through the inductor rises and builds up. In **Mode 2**, *S3* is turned off. At this time, the current path is formed as shown in **FIGURE 8** (b). The terminal voltage of inductor becomes V_{IN}-V_{OUT}. Since V_{IN}-$V_{OUT} > 0$, the current flowing through the inductor rises and energy builds up. However, the slope of the inductor current rise in **Mode 2** is smaller than in **Mode 1**, because $V_{IN} > V_{IN}$-V_{OUT}. In **Mode 3**, *S4* is turned on. At this time, the current path is formed as shown in **FIGURE 8** (c). Although *S4* changes from the turn-off to the turn-on state, energy passes through S4 in the same way as in **Mode 2**. Therefore, the voltage and current across the inductor are the same as in **Mode 2**. In **Mode 4**, *S1* is turned off. At this time, the current path is formed as shown in **FIGURE 8** (d). The terminal voltage of inductor becomes $-V_{OUT}$. The current flowing through the inductor decreases. In **Mode 5**, *S2* is turned on. At this time, the current path is formed as shown in **FIGURE 8** (e). Although *S2* changes from turn-off to turn-on, energy passes through S2 is the same as in **Mode 4**. Therefore, the voltage and current across the inductor are the same as in **Mode 4**. In **Mode 6**, *S2* and *S4* are turned off. At this time, the current path is formed as shown in **FIGURE 8** (f). Energy stored in the inductor still remains. Although *S2* and *S4* turn off from turn-on, the body diodes of *S2* and *S4* turn on due to the remaining energy in the inductor.

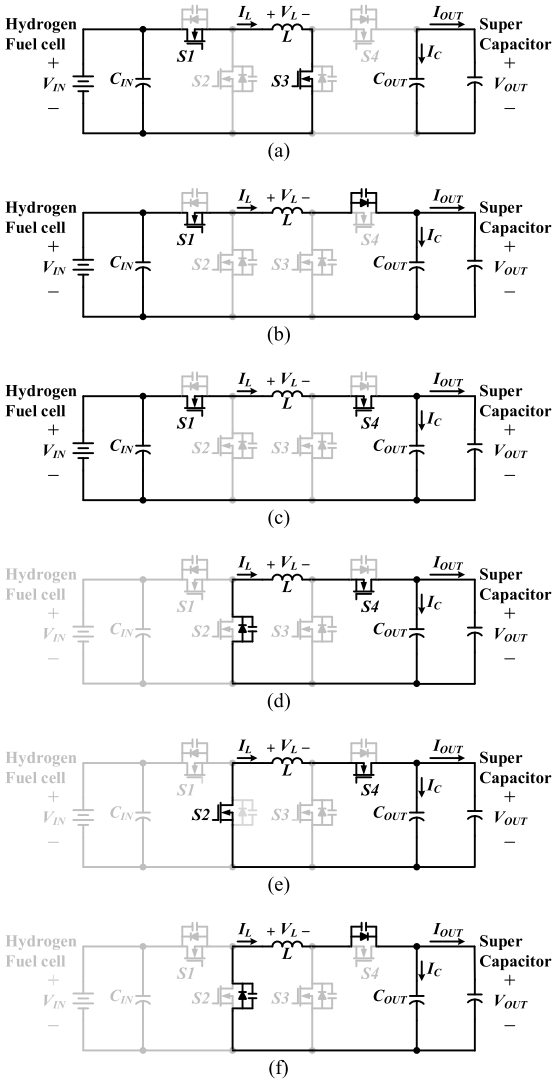

FIGURE 8. Energy path of FSBB converter with a novel control method (a) Mode 1, (b) Mode 2, (c) Mode 3, (d) Mode 4, (e) Mode 5, (f) Mode 6.

The energy passes through S2 and S4, which is the same as **Mode 5**. Thus, the voltage and current across the inductor are the same as in **Mode 5**. In buck operation and buck-boost operation, $G_{V,Buck}$ and $G_{V,Buck-boost}$ operation can be expressed through flux-balance as shown in Eq (4).

$$\frac{V_{OUT}}{V_{IN}} = \frac{D_F - D_d}{1 - (D_R - D_d)} \tag{4}$$

Upon reaching a critical threshold voltage, it enters the buck-boost operation region. At the transition point, by maintaining the D_F of the buck-boost operation at the same level as the D_F in the buck operation and linearly increasing only D_R, it satisfies the voltage gain requirement. Therefore, it enables more stable operation compared to the conventional control method.

B. SIMULATION

FIGURE 9 shows the simulation result applying the proposed control method in the condition; V_{IN} is 800V, V_{OUT} ranging from 0 to 800V, and I_{OUT} is 12.5A. The voltage ripple does not occur at the transition point.

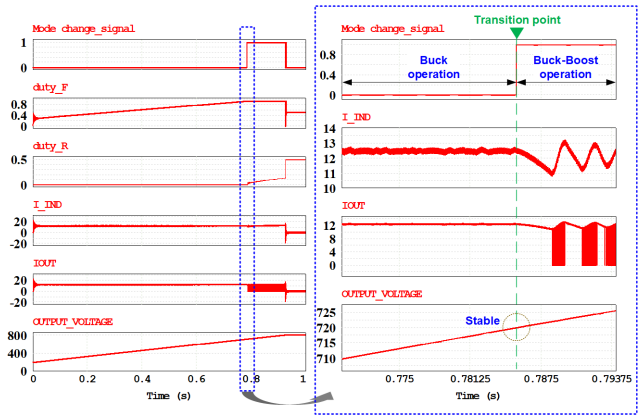

FIGURE 9. Simulation result at the transition point of the FSBB converter with a novel control method.

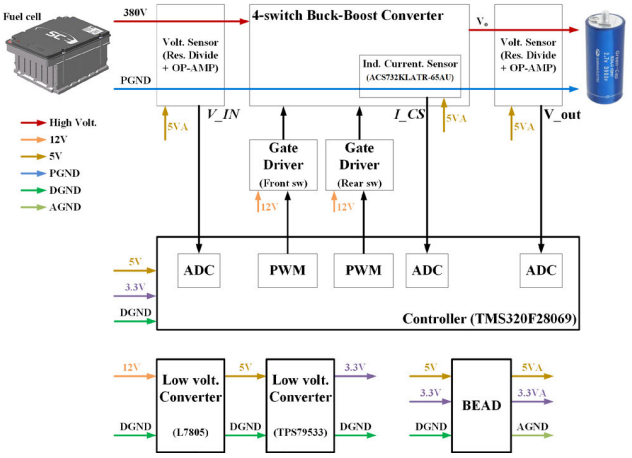

FIGURE 10. System block diagram of SCPC.

The components of the FSBB converter were applied as ideal models. The characteristics of the ideal models of the components used in the configuration are as follows:

- ESR and ESL for C_{IN} and C_{OUT} is 0.
- The insulation resistance of C_{IN} and C_{OUT} is infinite.
- The conductance of the winding for the inductor is infinite.
- The conductance of the power switch is infinite.
- Parasitic capacitance of the power switch is ignored.

The simulation results of the FSBB converter with the mentioned features are shown in **FIGURE 9**. The left waveform in **FIGURE 9** shows the entire interval from the initial state of the super capacitor to the fully charged state. The right waveform in **FIGURE 9** shows the time-expanded operation of the FSBB converter near the transition point. The signal named Mode Change_signal shows the mode transition point of FSBB converter. It produces 0 for buck operation, and 1 for buck-boost operation. Each signal

$$D_{F,\max} = 1 - f_s T_{OFF,\min} \tag{5}$$

$$L_{NOVEL} = \frac{D_{F,max}\left(1 - D_{F,max}\right) V_{IN}}{(1 - D_R) f_S \Delta I_L} \tag{6}$$

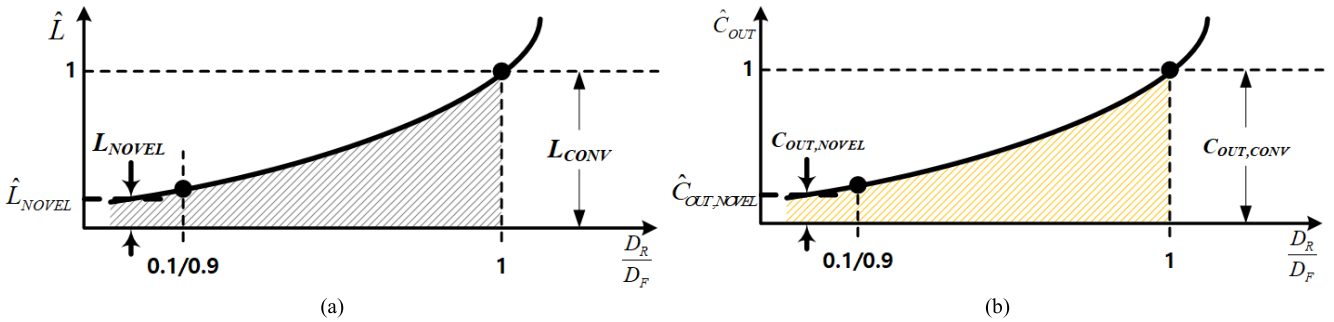

FIGURE 11. Required capacity curves of passive components with proposed control method (a) inductance normalized by L_{conv} and (b) capacitance normalized by $C_{OUT,conv}$.

TABLE 3. Input and output specifications of the FSBB converter.

Parameters	Values
V_{IN}	800V
V_{OUT}	0 ~ 800V
I_{OUT}	12.5A
Ripple of V_{OUT}	1% of V_{OUT}
Ripple of I_L	10% of I_{OUT}
Charging time	120sec
Switch component cooling	Water cooling
Efficiency	More than 90%

$$C_{OUT,NOVEL} = \frac{\left(1 - D_{F,max}\right) I_{OUT}}{f_S \Delta V_{OUT}} \tag{7}$$

$$L_{CONV} = \frac{D_{F,max} V_{IN}}{f_S \Delta I_L} \tag{8}$$

$$C_{OUT,CONV} = \frac{D_{F,max} I_{OUT}}{f_S \Delta V_{OUT}} \tag{9}$$

$$\widehat{L} = \frac{L_{NOVEL}}{L_{CONV}} = 1 - D_{F,max} \tag{10}$$

$$\widehat{C} = \frac{C_{OUT,NOVEL}}{C_{OUT,CONV}} = \frac{D_R}{D_F} \tag{11}$$

represents as follows: I_IND is current flowing through the inductor, IOUT is output current that is the current flowing into super capacitor, and OUTPUT_VOLTAGE is output voltage that is the voltage of the super capacitor.

There is no ripple in the OUTPUT_VOLTAGE at the transition point. It is anticipated that the proposed control method is able to stabilize the supercapacitor voltage at the transition point.

IV. HARDWARE DESIGN

A. DESIGN OVERVIEW

TABLE 3 is the electrical specifications of the SCPC designed in this paper. The SCPC is designed as the block diagram shown in **FIGURE 10**. The control system is implemented with TMS320F28069 microcontroller being powered by 12V battery of the HFCEV. In order to determine the start and end of SCPC operation and to control the output current, input voltage, output voltage, and current are sensed.

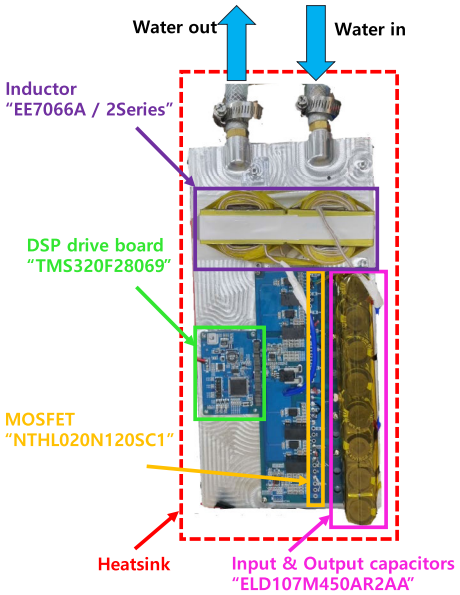

FIGURE 12. Prototype of SCPC.

TABLE 4. Summary of selected and designed components.

Components	Parameters	Values (Spec.)
Duty	$D_{F,max}$	0.9
Inductor	Total inductance	3.8mH
	Switching frequency	75kHz
	Core	EE7066 (2S)
	Wire	0.1phi/250strands/80turns
I/O capacitors	ELD107M450AR2AA	100F/450V (2P2S)
MOSFET	NTHL020N120SC1	1200V/103A (@25°C)

B. OPTIMAL COMPONENT DESIGN

The FSBB converter operates in two mode, buck and buck-boost with proposed control. The optimal period of each mode for SCPC can be designed by considering the electrical specification listed in TABLE 3. The parameters that need to be determined are as follows:

- The ratio of D_R to $D_{F,max}$ ($D_R/D_{F,max}$)
- The minimum turn-off time ($T_{OFF,min}$)
- Switching frequency. (f_S)

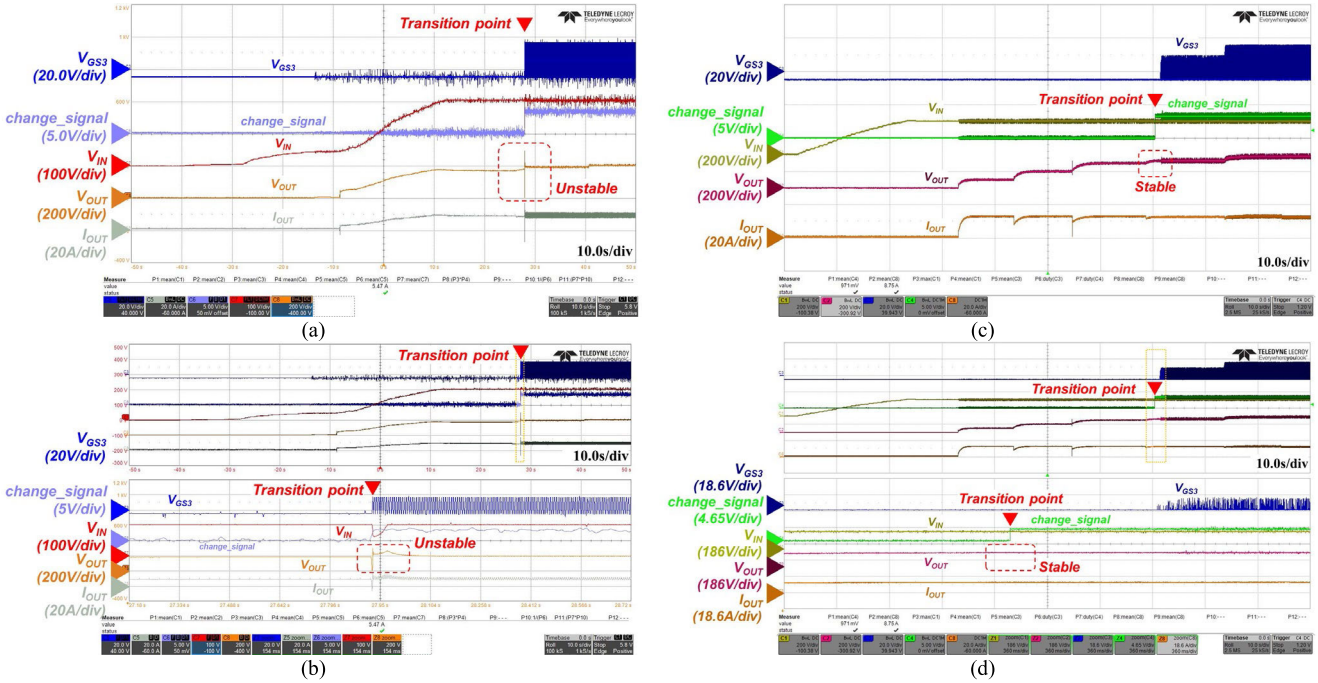

FIGURE 13. Waveforms of the SCPC with conventional and proposed control (a) V_{IN} = 200V, I_{OUT} = 8A with conventional control, (b) time-expanded waveform of (a) @transition point, (c) V_{IN} = 200V, I_{OUT} = 12.5A with proposed control, (d) time-expanded waveform of (c) @transition point.

In buck operation, output voltage is controlled by D_F only. In other words, the period of buck operation mode is determined by D_F, and also the transition point of operation mode is delayed according to D_F. For buck-boost mode, it is required to secure turn-off time because of rise and falling time of switch. Thus, the maximum value of D_F is affected by switching frequency and the minimum value of turn-off time as shown in Eq. (5).

The larger $D_{F,max}$, the higher power density. In other words, the volume of the inductor and output capacitor is able to be minimized by setting $D_{F,max}$ as high as possible. It means that the later the transition point, the smaller the volume of inductor and output capacitor. The inductance and capacitance can be calculated according to Eq (6) and (7).

With conventional control method, the desirable value of L_{CONV} and $C_{OUT,CONV}$ are able to be calculated by Eq (8) and (9). The **FIGURE 11** shows that the curves of L and C_{OUT} according to the ratio of D_R to D_F. With conventional control method, the D_F and D_R are equal value in buck-

$$D_{F,max} + D_{R,max} = 1 \tag{12}$$

$$C(D_R) = \frac{D_R I_{OUT}}{f_S \Delta V_{OUT}} \tag{13}$$

boost operation, which means that D_R/D_F is 1. $\hat{L}_{NOVEL}$ and $\hat{C}_{OUT,NOVEL}$ represent the normalized values by L_{CONV} and $C_{OUT,CONV}$ respectively. They can be expressed by Eq (10) and (11). $D_R/D_{F,max}$ can be determined based on the trends of $\hat{L}$ and $\hat{C}_{OUT}$.

In order to plot the curves of $\hat{L}$ and $\hat{C}_{OUT}$ as shown in **FIGURE 11**. the following five assumptions are required:

- Input voltage is fixed.
- Output current is fixed.
- Output voltage ripple is constant.
- f_S is fixed.
- D_d is ignored.
- Inductor current ripple is constant.

The curve in **FIGURE 11** shows that required inductance and capacitance decrease as $D_{F,max}$ increases. In order to minimize the size of the inductor and output capacitor, it is required to design $D_{F,max}$, as high as possible.

In order to select the capacitance, Eq (12) and (13) for buck-boost operation can be derived. Eq (13) has the maximum capacitance in buck-boost operation when D_F is 0.1 or when D_R is 0.9. Because, if sum of D_F and D_R is larger than 1, output voltage of FSBB converter becomes higher than input voltage of FSBB converter. However, voltage gain of FSBB converter acting SCPC cannot be higher than 1. Both equations yield the maximum capacitance for their respective condition. Through Eq (12) and (13), capacitance value that satisfies the specification in TABLE 3.

V. EXPERIMENTAL RESULTS

FIGURE 12 shows the manufactured prototype with the components listed in TABLE 4. The experimental results are shown in **FIGURE 13**. The waveforms are obtained by applying the conventional control method and the proposed one.

The change_signal is generated by TMS320F28069. When the FSBB converter operates in buck mode, the signal level is low state(0V). In buck-boost mode, it is high state (3.3V).

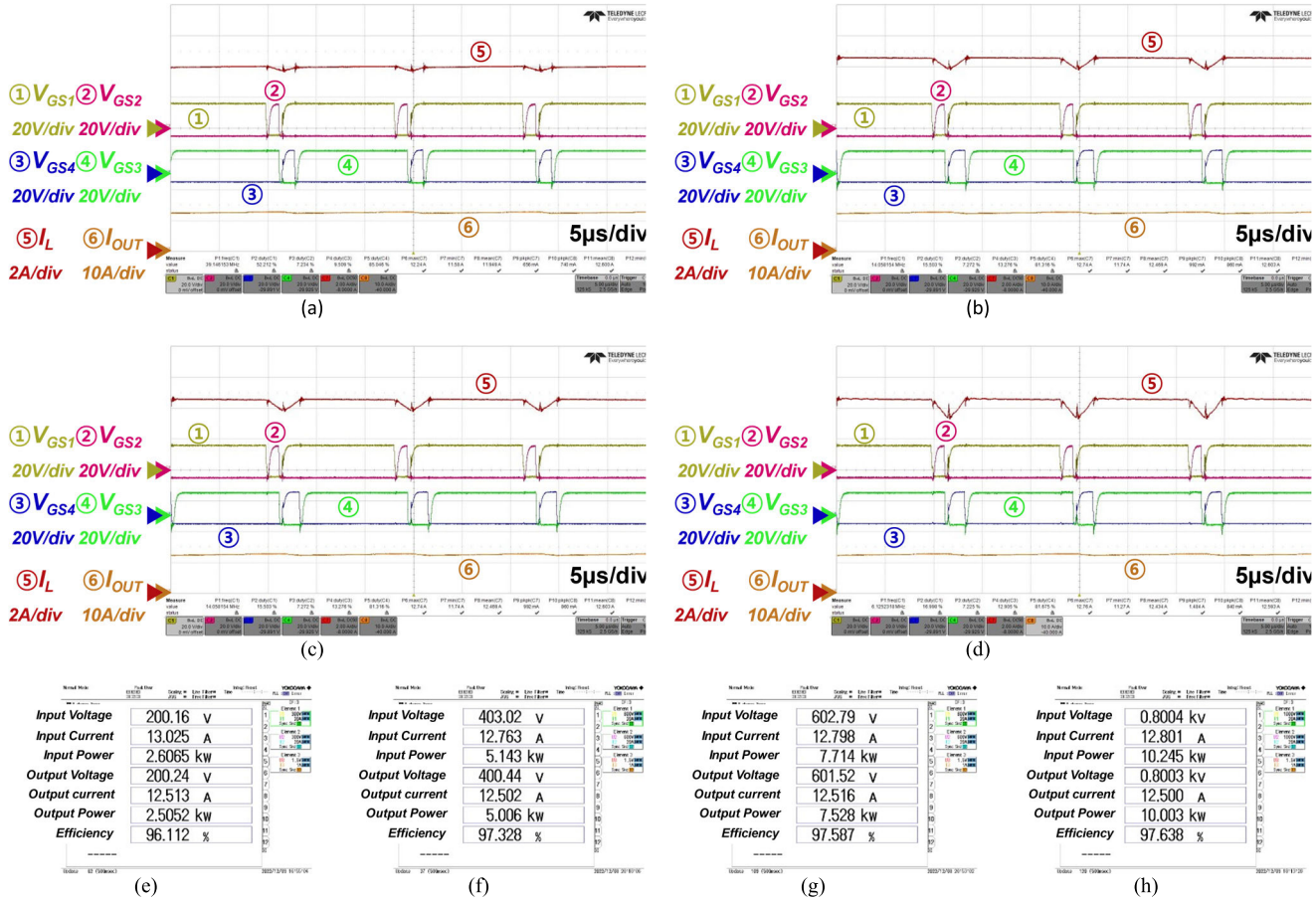

FIGURE 14. Experimental result at gain of SCPC that is about 1 (a),(e) V_{IN} = 200V,V_{OUT} = 200V,I_{OUT} = 12.5A, (b), (f)V_{IN} = 400V,V_{OUT} = 400V,I_{OUT} = 12.5A, (c), (g)V_{IN} = 600V,V_{OUT} = 600V,I_{OUT} = 12.5A, (d),(h) V_{IN} = 800V,V_{OUT} = 800V,I_{OUT} = 12.5A.

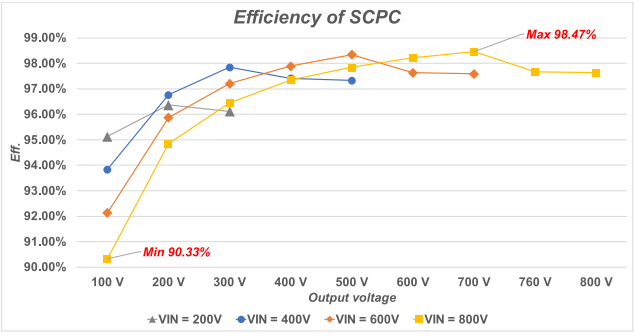

FIGURE 15. Efficiency curve of SCPC.

V_{GS3} is the gate signal of S3, V_{IN} and V_{OUT} are the input and output voltage of the SCPC, respectively. I_{OUT} is the charging current.

Comparing the both waveforms, the output voltage ripple is reduced at the transition point where the change_signal shifts from low to high state. From the result, it is verified that FSBB converter is able to overcome regulation problem at transition point with proposed control method.

In order to conduct experiments in this paper, the SCPC was powered by a DC source, and the output was connected to the Electronic Load (E/L) for experimentation using CR mode. Since the SCPC is controlled by CC, if the CR is increased linearly, the output voltage of the SCPC will increase linearly. SCPC that is used conventional control method is controlled to output 8A current. Because used DC source has operation current specification that is 19Amax. In transition point then conventional buck-boost mode, duty is about 70% caused by duty loss. At this time, required input current magnitude is about 29A. However, used DC source cannot supply it. It already was predicted this limitation. Accordingly, SCPC that is used conventional control method is tested with 8A output current. Therefore, the experimental method employed in this paper can be considered analogous to the charging of a super capacitor. The experiments were conducted by increasing the E/L while observing the output voltage waveform at the transition point.

Furthermore, it was confirmed that the SCPC can operate normally after the transition point at the maximum output point through the proposed control method, as shown in **FIGURE14**. **FIGURE 14** (a), (b), (c), and (d) represent the operational waveform at V_{IN}/V_{OUT} = 1 of the SCPC, and **FIGURE 14** (e), (f), (g), and (h) shows the actual measured power analysis data.

Additionally, considering the voltage drop in the hydrogen fuel cell when charging the super capacitor, the operational

efficiency at various input voltage was verified. The result is efficiency curve as shown in FIGURE 15. The minimum efficiency is approximately 90.33%, satisfying the target efficiency of 90% or higher as stated in TABLE 3.

VI. CONCLUSION

In this paper, FSBB converter with conventional control method was analyzed. It has output voltage regulation problem at transition point. It is because there is non-linearity between $G_{V,Buck}$ and $G_{V,Buck-boost}$ curve. In order to overcome the problem, a novel control scheme is proposed for the FSBB converter. It is proposed to depart from the existing pair framework and introduce a novel approach to forming continuity between $G_{V,Buck}$ and $G_{V,Buck-boost}$ at the transition point. The feasibility of the proposed control method is validated by simulation and experiment with prototype.

REFERENCES

[1] S.-C. Ma, J.-H. Xu, and Y. Fan, "Characteristics and key trends of global electric vehicle technology development: A multi-method patent analysis," *J. Cleaner Prod.*, vol. 338, Mar. 2022, Art. no. 130502.
[2] G. Wang, Z. Xu, F. Wen, and K. P. Wong, "Traffic-constrained multiobjective planning of electric-vehicle charging stations," *IEEE Trans. Power Del.*, vol. 28, no. 4, pp. 2363–2372, Oct. 2013.
[3] L. Li, Z. Huang, H. Li, and H. Lu, "A high-efficiency voltage equalization scheme for supercapacitor energy storage system in renewable generation applications," *Sustainability*, vol. 8, no. 6, p. 548, Jun. 2016.
[4] I. H. Panhwar, K. Ahmed, M. Seyedmahmoudian, A. Stojcevski, B. Horan, S. Mekhilef, A. Aslam, and M. Asghar, "Mitigating power fluctuations for energy storage in wind energy conversion system using supercapacitors," *IEEE Access*, vol. 8, pp. 189747–189760, 2020.
[5] A. Kaknevicius and A. Hoover, "Managing inrush current," Texas Instrum., Dallas, TX, USA, Appl. Rep. 8, Aug. 2015, pp. 1–13.
[6] Y. Zhang, W. Zhang, F. Gao, S. Gao, and D. J. Rogers, "A switched-capacitor interleaved bidirectional converter with wide voltage-gain range for super capacitors in EVs," *IEEE Trans. Power Electron.*, vol. 35, no. 2, pp. 1536–1547, Feb. 2020.
[7] M. Venkatesh Naik and P. Samuel, "A non-inverting multi device interleaved buck boost converter for fuel cell low voltage applications," in *Proc. Global Conf. Advancement Technol. (GCAT)*, Oct. 2019, pp. 1–7.
[8] P. Andrade, F. Bento, A. N. Alcaso, and A. J. M. Cardoso, "Comparative study of single-switch and double-switch converter topologies, working on dead-zone mode, for fuel cell applications," in *Proc. 2nd Int. Conf. Sustain. Mobility Appl., Renewables Technol. (SMART)*, Nov. 2022, pp. 1–6.
[9] S. K. Kollimalla, M. K. Mishra, and N. L. Narasamma, "Design and analysis of novel control strategy for battery and supercapacitor storage system," *IEEE Trans. Sustain. Energy*, vol. 5, no. 4, pp. 1137–1144, Oct. 2014.
[10] S. Krishnaveni and M. Rasu, "Analysis of four switch positive buck boost converter based on mode selection circuit for portable battery applications," in *Proc. IEEE Sponsored 2nd Int. Conf. Innov. Inf. Embedded Commun. Syst.*, 2015, pp. 16571–16576.
[11] Y.-J. Lee, A. Khaligh, and A. Emadi, "A compensation technique for smooth transitions in a noninverting buck–boost converter," *IEEE Trans. Power Electron.*, vol. 24, no. 4, pp. 1002–1015, Apr. 2009.
[12] L. Callegaro, M. Ciobotaru, D. J. Pagano, E. Turano, and J. E. Fletcher, "A simple smooth transition technique for the noninverting buck–boost converter," *IEEE Trans. Power Electron.*, vol. 33, no. 6, pp. 4906–4915, Jun. 2018.
[13] X. Weng, Z. Zhao, K. Chen, L. Yuan, and Y. Jiang, "A nonlinear control method for bumpless mode transition in noninverting buck–boost converter," *IEEE Trans. Power Electron.*, vol. 36, no. 2, pp. 2166–2178, Feb. 2021.
[14] M. Duan, D. Sun, J. Duan, L. Sun, and Y. Liu, "Interleaved modulation scheme with optimized phase shifting for double-switch buck–boost converter," *IEEE Access*, vol. 9, pp. 55422–55435, 2021.
[15] J. Fang, X. Ruan, X. Huang, R. Dong, X. Wu, and J. Lan, "A PWM plus phase-shift control for four-switch buck–boost converter to achieve ZVS in full input voltage and load range," *IEEE Trans. Ind. Electron.*, vol. 69, no. 12, pp. 12698–12709, Dec. 2022.
[16] Y. Bai, S. Hu, Z. Yang, Z. Zhu, and Y. Zhang, "Model predictive control for four-switch buck–boost converter based on tuning-free cost function with smooth mode transition," *IEEE J. Emerg. Sel. Topics Power Electron.*, vol. 10, no. 6, pp. 6607–6618, Dec. 2022.
[17] X. Li, Y. Liu, and Y. Xue, "Four-switch buck–boost converter based on model predictive control with smooth mode transition capability," *IEEE Trans. Ind. Electron.*, vol. 68, no. 10, pp. 9058–9069, Oct. 2021.

HYEON-JUN KWON received the B.S. degree in electronic engineering and the M.S. degree in electrical and electronic convergence system engineering from Keimyung University, Daegu, South Korea, in 2021 and 2024, respectively. His current research interests include plasma generation power supply, portable ESS dc–ac inverter, battery management systems, and power converters for hydrogen fuel cell applications.

KU-YONG KIM received the B.S. degree in electronics engineering from Kyonggi University, Suwon, South Korea, in 2008. He is currently pursuing the Ph.D. degree with the Department of Electric Energy Engineering, Daegu Catholic University, Daegu, South Korea. From 1995 to 2011, he was an Engineer with the Power Division, Samsung-Electronics Company, Suwon. Since 2011, he has been the CEO of MDM, Daegu. His research interests include printed circuit board (PCB) technology, battery chargers for electric vehicles, and battery packs.

JUN-HO KIM received the B.S., M.S., and Ph.D. degrees in electrical engineering from Korea Advanced Institute of Science and Technology (KAIST), Daejeon, South Korea, in 2009, 2011, and 2016, respectively. From 2016 to 2017, he was a Senior Research Engineer with Hyundai Motors Company, Hwaseong, South Korea, where he was involved in the development of an EV battery charger. He is currently an Associate Professor with the Department of Electrical Energy Engineering, Keimyung University, Daegu, South Korea. His current research interests include battery chargers for electric vehicles, resonant converters, distributed power systems, digital control approaches for dc–dc converters, battery management systems, and power converters for hydrogen fuel cell applications.